In vivo Ca^{2+} imaging in the endoplasmic reticulum with an optimized GFP-aequorin sensor

Abbreviated Title: Ca^{2+} imaging of endoplasmic reticulum *in vivo*

Paloma Navas-Navarro[a,1], Jonathan Rojo-Ruiz[a,1], Macarena Rodriguez-Prados[a], María Dolores Ganfornina[a], Loren L. Looger[b], María Teresa Alonso[a,2] and Javier García-Sancho[a,2]

[a]Instituto de Biología y Genética Molecular (IBGM), University of Valladolid and CSIC, Valladolid, Spain.

[b]Howard Hughes Medical Institute, Janelia Research Campus, Ashburn, Virginia, USA.

[1]These authors contributed equally to this work.

[2] To whom correspondence may be addressed. Email: talonso@ibgm.uva.es or jgsancho@ibgm.uva.es

Corresponding author: María Teresa Alonso (talonso@ibgm.uva.es) or Javier Garcia-Sancho (jgsancho@ibgm.uva.es). Instituto de Biología y Genética Molecular (IBGM). Universidad de Valladolid y Consejo Superior de Investigaciones Científicas. c/ Sanz y Forés 3. 47003 Valladolid, Spain.

Phone: +34 983 423084; Fax: +983 184800

Abbreviations: GAP, GFP-Aequorin Protein; ER, endoplasmic reticulum; SR, sarcoplasmic reticulum; SERCA, sarco-endoplasmic reticulum Ca^{2+} ATPase; TBH, tert-butyl-hidroquinone; GECI, genetically encoded calcium indicator; GFP, green fluorescent protein; $[Ca^{2+}]_C$, $[Ca^{2+}]_{ER}$, $[Ca^{2+}]_{SR}$, $[Ca^{2+}]_{GO}$, Ca^{2+} concentrations in cytosol, ER, SR or Golgi apparatus, respectively. CICR, Ca^{2+}-induced Ca^{2+}-release.

ABSTRACT

Proper functioning of organelles such as the endoplasmic reticulum (ER) or the Golgi apparatus requires luminal accumulation of Ca^{2+} at high concentrations. Genetically encoded Ca^{2+} indicators are invaluable tools for monitoring intra-organellar Ca^{2+} signals *in vitro*, but the presently available sensors have proven to be of limited value for *in vivo* use. Here we describe a low affinity Ca^{2+} sensor of the GFP-Aequorin Protein (GAP) family optimized for measurements in high Ca^{2+} concentration environments. This indicator is ratiometric, insensitive to Mg^{2+} and to pH, and easy to calibrate. It can be used in combination with other indicators for simultaneous imaging of ER and cytosolic Ca^{2+}. We generated transgenic animal models (flies and mice) for the improved GAPs targeted to the ER, where functional Ca^{2+} transients could readily be detected. The utility of the ER sensor was demonstrated under three experimental paradigms: i) ER Ca^{2+} oscillations in cultured astrocytes, ii) *ex vivo* functional mapping of ER cholinergic receptors in acute hippocampal slices from transgenic mice, and iii) *in vivo* sarcoplasmic reticulum Ca^{2+} dynamics in the muscle of transgenic flies. Our results provide proof of concept for the suitability of the new biosensors to monitor Ca^{2+} dynamics inside intracellular organelles under physiological conditions and open an avenue to explore complex Ca^{2+} signalling in animal models of health and disease.

Keywords: biosensor, calcium, organelles, GFP, aequorin, GECI, endoplasmic reticulum, Golgi apparatus.

SIGNIFICANCE STATEMENT

Intracellular organelles such as the endoplasmic reticulum (ER) or the Golgi apparatus require luminal accumulation of Ca^{2+} at high concentrations for proper functioning. Direct intra-organellar measurement of Ca^{2+} concentrations in intact preparations is essential to address complex physiological questions. Few genetically encoded Ca^{2+} indicators have been developed for high-Ca^{2+} organelles, and none of these have been used *in vivo* in the context of transgenic expression. We describe a new Ca^{2+} sensor of the GFP-Aequorin Protein (GAP) family designed to accurately monitor Ca^{2+} concentration in high-Ca^{2+} environments. Expression of the sensor in the endoplasmic reticulum in neurons and muscle of transgenic animal models (flies and mice) enabled to monitor fast physiological responses under minimally disturbing conditions *ex vivo* and *in vivo*. This sensor provides a valuable tool to explore subcellular complex Ca^{2+} signalling *in vivo* in animal disease models.

INTRODUCTION

Maintenance of high [Ca^{2+}] in the lumen of Ca^{2+} storage organelles, such as the endoplasmic reticulum (ER) or the Golgi apparatus (Go), is crucial for their correct functioning. Chronic decrease of $[Ca^{2+}]_{ER}$ triggers ER stress and the "unfolded protein response" (Gallego-Sandin, et al., 2011), whereas reduction of $[Ca^{2+}]_{GO}$ disturbs segregation and cargo sorting (Kienzle and von Blume, 2014). Direct and calibrated measurements of intraluminal Ca^{2+} levels are imperative to understand Ca^{2+} responses underlying different physiological and pathophysiological conditions. In the past decade an increasing number of genetically encoded Ca^{2+} indicators (GECIs) have been developed. Most of them have been engineered to have high Ca^{2+} affinity and only a few for use in high [Ca^{2+}] environments (Henderson, et al., 2015; Palmer and Tsien, 2006; Suzuki, et al., 2014; Tang, et al., 2011; Wu, et al., 2014). Although some indicators have been expressed in transgenic animals, its utility has proven problematic, displaying small responses, probably due to the interaction of the sensor with endogenous partners. Furthermore, to date there are no reports on the *in vivo* use of transgenic low-Ca^{2+} affinity indicators.

We have recently described a new family of fluorescent Ca^{2+} sensors named GAP (for GFP-Aequorin Protein) (Rodriguez-Garcia, et al., 2014). A unique feature of this family is the use of aequorin instead of calmodulin or troponin-C to provide the Ca^{2+} binding sites. This makes much less likely the association of the indicator with endogenous proteins ("bio-orthogonality"), thus avoiding possible interferences. Other advantages of the GAP sensors include its ratiometric capability and its targetability to various organelles. The first low Ca^{2+} affinity GAP variant, named GAP1, displays an apparent dissociation constant value for Ca^{2+} (K_d) of 16 μM, much

lower than other GECIs. GAP1 is valuable for measuring, for example, in the low-Ca^{2+} subcompartment of the Golgi apparatus (Aulestia, et al., 2015), but still far below the resting $[Ca^{2+}]_{GO}$ in the high-Ca^{2+} subcomparment or the $[Ca^{2+}]_{ER}$, that are in the range of 250 to 600 μM (Alonso, et al., 1998; Aulestia, et al., 2015).

Here we report the development of new low affinity Ca^{2+} sensors (GAP2 and GAP3) optimized for imaging Ca^{2+} dynamics in vivo in high Ca^{2+} organelles. We demonstrate their use for $[Ca^{2+}]_{ER}$ monitoring under various experimental settings, including ER-Ca^{2+} oscillations in cultured astrocytes; ER-Ca^{2+} release by acetylcholine hippocampal slices *ex vivo;* and muscle of transgenic flies *in vivo.* .

RESULTS AND DISCUSSION

Optimization of GAP for measuring in high $[Ca^{2+}]$ environments

Because of its relatively high affinity for Ca^{2+}, the previously described ER-targeted GAP1 (erGAP1) only poorly detected small changes of $[Ca^{2+}]_{ER}$, although it was valuable for measurements of large variations in luminal Ca^{2+} (Fig. 1a). We therefore introduced new substitutions in the EF hands of aequorin to further decrease GAP affinity for Ca^{2+}. Of the 22 mutants tested (Table S1) the double mutant D24N/D119A (named GAP2) displayed a K_d of 407 μM (Fig. 1b), well suited for measuring $[Ca^{2+}]_{ER}$. As a consequence, the sensitivity of the improved ER-targeted GAP2 (erGAP2) to detect submaximal ER calcium releases was greatly increased with respect to erGAP1 (Fig. 1a).

Further optimization of the indicator included humanization of GAP2 codon usage to improve expression in mammals and re-engineering of various residues in the GFP

moiety to increase its fluorescence intensity (Table S2). The brightest functional variant (named GAP3) contained the substitutions S175G, D180Y, I167V and L15Q and exhibited a K_d of 489 μM. Importantly, the dynamic range (~3-fold) was not substantially altered with respect to the parental GAP1. Both GAP2 and GAP3 behaved very similarly and were used interchangeably in the following experiments. Remarkably, these sensors possess a Hill coefficient (n) of 1.0 (Fig. 1b); it is likely that two out of the three Ca^{2+}-binding sites in aequorin have been rendered non-functional in GAP, while preserving the fluorescence signalling mechanism. Sensors with higher Hill coefficients are more difficult to calibrate (Suzuki, et al., 2014). Furthermore, GAP is practically insensitive to variations in Mg^{2+} concentration (in the 0.1 to 5 mM range; Fig. S1a) or pH (in the 6.5 to 8.5 pH range; Fig. S1b). At lower pH values the apparent affinity for Ca^{2+} decreased (the K_d increased 2.4 times at pH 6 and 40 times at pH 5.5; Fig. S1b).

Accurate measurement of luminal [Ca^{2+}] requires satisfaction of several criteria: high signal-to-noise ratio, large dynamic range with a midpoint close to resting [Ca^{2+}], and reliable *in situ* calibration. We targeted GAP3 to the ER (erGAP3); erGAP3 was bright and co-localized with ER markers. Cell stimulation with ATP produced large, coordinated changes in the fluorescences excited at 405 and 470 nm (Fig. 1c). Complete emptying of the ER resulted in F_{min}, that was obtained by stimulation in Ca^{2+}-free medium containing the reversible sarco-endoplasmic reticulum Ca^{2+} ATPase (SERCA) inhibitor tert-butylhydroquinone (Moore, et al., 1990) (TBH, Fig. 1c). Similar results were obtained with the irreversible SERCA blocker thapsigargin (Thastrup, et al., 1989), although in this case ER stores did not refill after inhibitor washout (Fig. S2a). Finally, we calibrated erGAP3 response against the cytoplasmic

Ca^{2+}-sensitive dye Rhod-3, whose red fluorescence was easily separable from GAP3 (Fig. 1d, shown together with the erGAP3 R/R_0 ratio values). Interestingly, comparison of Ca^{2+} kinetics in the two compartments revealed that the cytosolic Ca^{2+} peak preceded the ER Ca^{2+} decrease peak (Fig.1d). erGAP3 was also calibrated against Fura-2 (Fig. S2b) with similar results. These findings indicate that $[Ca^{2+}]_C$ changes only crudely correlate with $[Ca^{2+}]_{ER}$ changes and direct ER measurements are required for precise description of Ca^{2+} kinetics in this compartment.

Oscillations of $[Ca^{2+}]_{ER}$ in cultured cortical astrocytes

We next applied the new sensors to explore various aspects of ER Ca^{2+} dynamics under three experimental paradigms. In the first setting we expressed the ER-targeted sensor in cortical astrocytes by infecting primary cultures with an erGAP2 Herpes viral vector (Fig. 2). The indicator successfully reported $[Ca^{2+}]_{ER}$ dynamics and was sensitive enough to follow Ca^{2+} oscillations inside the ER. Stimulation with ATP, which induces Ca^{2+} release from the ER via inositol trisphosphate (Verkhratsky, et al., 2012), reduced the GAP fluorescence (R/R_0) by about 50% (Fig. 2a). In these cells, low extracellular $[K^+]$ induces Ca^{2+} entry and triggers oscillations of the cytosolic Ca^{2+} (Dallwig, et al., 2000). We demonstrate here that the cytosolic oscillations are due to large $[Ca^{2+}]_{ER}$ oscillations that could be directly recorded with erGAP2 (video 1). The entry of Ca^{2+} across the plasma membrane would firstly trigger a Ca^{2+} release from the ER via activation of the ryanodine receptor (RyR) through a process of Ca^{2+}-induced Ca^{2+}-release (CICR) (Alonso, et al., 1999). The luminal depletion will then desensitize the RyR and promote the gradual Ca^{2+} loading of the ER. As soon as the luminal Ca^{2+} reached a threshold, it would sensitize the RyR such that it starts to release Ca^{2+} again.These regular cycles of Ca^{2+} release and uptake across the ER

membrane will operate as long as the Ca^{2+} flowing into the cell is guaranteed by the continuous low extracellular [K^+] stimulation.

Additionally, detailed analysis of the probe signal enabled us to investigate how $[Ca^{2+}]_{ER}$ oscillations are propagated from cell to cell. The lower panel in Fig. 2a shows details of the cell to cell progression. It seems clear that cell excitation, understood here as the progression of the Ca^{2+} release from the ER, was able to jump from one cell to its neighbour (arrowheads in Fig. 2a). The main wave was visible in the average trace of all the cells present in the field (n=7; Fig. 2b), indicating some degree of synchronization.

Functional mapping of ER Ca^{2+} responses to neurotransmitters in hippocampal slices *ex vivo*

We next generated lines of transgenic mice expressing erGAPs (2 and 3) under the ubiquitous *CAG-GS* promoter (Fig. S3a). Hippocampus showed strong expression of the sensors (Fig. S3b). We looked for functional responses to neurotransmitters in the different areas of the hippocampus examined at low magnification using acute slices from erGAP3 transgenic mice. ER- and cytosolic-Ca^{2+} dynamics were simultaneously monitored using erGAP3 and Rhod-3, respectively (Fig. 3). ER Ca^{2+} release in response to acetylcholine selectively occurred in the CA1 region (Fig. 3a). These results correlate well with the expression of the muscarinic acetylcholine receptors (Fernandez de Sevilla, et al., 2008; Power and Sah, 2002). Interestingly, a detailed comparison between $[Ca^{2+}]_C$ and $[Ca^{2+}]_{ER}$ kinetics (Fig. 3b) showed that maximal $[Ca^{2+}]_C$ rise preceded maximal ER release, in agreement with the results shown above in HeLa cells (Fig. 1d).

***In vivo* monitoring of Ca^{2+} release in the sarcoplasmic reticulum of fly muscle**

To demonstrate the feasibility of *in vivo* measurements with the new ER Ca^{2+} sensors, we genetically engineered *Drosophila* to express erGAP3 specifically in the sarcoplasmic reticulum (SR) of striated muscles (Fig. 4a and 4b). We investigated SR Ca^{2+} dynamics in the living fly by imaging GAP fluorescence in the thorax muscles during electrical stimulation of the giant fiber, a useful model system for studies of muscle function during nerve stimulation that permits simultaneous activation of all the motor nerves (Allen and Godenschwege, 2010). At low frequency (0.25-0.5 Hz), erGAP3 readily detected individual SR release events secondary to nerve stimuli, with small and repetitive decreases in F_{470} and concomitant rises in F_{405} (Fig. 4c). SR Ca^{2+} release was completed in less than 100 ms and was followed by a slower Ca^{2+} reuptake ($T_{1/2}$, 0.5 - 1 s) (Figs. 4c and S4a). At high frequency stimulation (4-16 Hz), individual SR-release events fused and summated during the first 1.5 s, resulting in a much larger release (Fig. 4d, S4b and S4c). We also generated transgenic flies expressing GCaMP3 in muscle to image cytosolic Ca^{2+} in parallel experiments. The decreases in $[Ca^{2+}]_{SR}$, imaged with erGAP3, correlated well with the large increases in $[Ca^{2+}]_C$, imaged with GCaMP3 (Fig. 4e). Taken together, these results demonstrate that the new sensor erGAPs enable to monitor SR-Ca^{2+} release dynamics in response to physiological stimulation with a high temporal resolution *in vivo*.

In summary, the optimized Ca^{2+} sensors represent a substantial improvement over previous GAPs due to its optimal K_d for measurements in high $[Ca^{2+}]$ compartments, its ratiometric measurements, large dynamic range and uncomplicated calibration (Rodriguez-Garcia, et al., 2014). Even more relevant is its bio-orthogonal nature,

which facilitates robust functional expression of the indicator with no apparent off-target effects. Finally, we demonstrate the applicability of the sensor, both *ex vivo* and *in vivo*, to address different aspects of subcellular Ca^{2+} homeostasis. Its use in combination with new disease models, such as those provided by iPS cell technology (Fernandez-Santiago and Ezquerra, 2016; Wan, et al., 2015), promises novel approaches to investigate the pathophysiological relevance of organellar Ca^{2+} dyshomeostasis.

MATERIALS AND METHODS

Gene construction

The original GAP containing the D119A substitution in aequorin (Rodriguez-Garcia, et al., 2014) was cloned in pcDNA3. The initial GAP gene library was constructed by site-directed mutagenesis (QuickChange Site-directed mutagenesis kit, Stratagene) using the oligonucleotides No. 1 to 22 listed in Table S3. Genes encoding GAP variants were sub-cloned into pET28a for expression, purification and screening in *E. coli*. The secondary GAP library (Table S2) was created using erGAP2 cloned in pcDNA3 as a template and oligonucleotides No. 23 to 29 of Table S3.

To target GAP2 or GAP3 to the ER (erGAP), the calreticulin signal peptide and the sequence encoding the ER-retention tag, KDEL, were fused in frame to the 5'- and the 3'-end, respectively, resulting in pcDNA3-erGAP2 and pcDNA3-erGAP3. To produce viral vectors, erGAP2 cDNA was cleaved from pcDNA3 as a HindIII/EcoRI fragment and cloned into the Herpes Simplex Virus plasmid pHSVpUC.

In order to improve gene expression in mouse, sequence optimization of the erGAP2 gene was performed (ATG:biosynthetics GmbH, Germany). To make transgenic mice, mammalian codon usage-optimized erGAP2 and erGAP3 were sub-cloned into the pCAG-GS vector with a *CAG* promoter (Miyazaki, et al., 1989) (CMV enhancer, β-actin promoter) and regulatory elements from the woodchuck hepatitis virus (WPRE; Fig. S3a). To make transgenic flies, erGAP3 was cloned into pUASt-attB vector (GenBank accesion No. EF362409). The integrity of all constructs was verified by sequencing.

Bacterial expression and protein purification

GAP variants in pET28a were transformed in *E. coli* BL21 (Stratagene). For protein expression, bacteria were grown at 37º C to A_{600} >0.6 in LB containing 40 mg/l kanamycin and induced with 0.5 mM isopropyl β-D-thiogalactoside (IPTG) for 6h at 25º. The cells were then pelleted by centrifugation at 6000 g for 10 min, and sonicated in a buffer containing (in mM): NaCl, 250; EDTA, 5; phenylmethylsulfonyl fluoride, 0.5; DTT (reducing agent), 2; Tris-HCl, 50, pH 8.8. The bacterial lysate was centrifuged at 30,000 g for 10 min. Most of the protein was present in inclusion bodies as an insoluble material that could be solubilized in 8 M urea, 5 mM DTT, 50 mM Tris-HCl, pH 8.8, by rocking at 4º overnight. The insoluble protein was removed by centrifugation at 30,000 g for 15 min. For small-scale cultures used for screening, protein in supernatant was refolded by filtration with 150 mM NaCl, 5 mM DTT, 50 mM Tris–HCl (pH 8.8) at 4º using a 10K filter (Amicon) in such a way that urea was 125-fold diluted. For Ca^{2+} titration of GAP2 or GAP3, urea was dialyzed against 50 mM Tris-HCl (pH 8.8) at 4º. Next, 5 mM DTT was added and proteins were further purified with Ni-Sepharose beads (GE Healthcare). Protein quantification was performed by the Bradford method.

GAP screening

Mutant screening (Table S1) was performed using a Tecan Genios Pro 96-well plate reader. GAP recombinant proteins (3 µg) were added to each well containing 200 µl of PBS, pH 7.4 at three different Ca^{2+} concentrations: 0 (0.1 mM EGTA added), 0.1 mM and 1 mM. GAP fluorescence was measured in triplicate at 390 and 485 nm excitation and 535 nm emission. These values were used to calculate the F_{485}/F_{390} ratio (which was similar to F_{470}/F_{405} ratio). Ratio values obtained with Ca^{2+} (0.1 and 1 mM Ca^{2+}) were divided by the ones obtained with EGTA (R_{Ca}/R_{EGTA}) and, finally, the values obtained with 1 mM Ca^{2+} were divided by the ones obtained with 0.1 mM Ca^{2+}. Only those GAP mutants that gave $R_{Ca1}/R_{Ca0.1}$ values larger than 1.5 were pursued. The secondary screening of GAP2 mutants was performed in transiently transfected HeLa cells.

Calibration with Ca^{2+} and interactions with H^{+} and Mg^{2+}

Measurements were performed in the plate reader (see above). Recombinant GAP proteins (3 µg) were added to each well with 200 µl of a buffer containing (in mM): KCl, 140; $MgCl_2$, 1; MOPS/Tris, 20, pH 7.2. Ca^{2+} calibrations were performed in Ca^{2+}-free medium (0.1 mM EGTA added), or in the same solutions containing increasing Ca^{2+} concentrations between 50 µM and 50 mM. R_{max} and R_{min} were computed as the F_{485}/F_{390} ratios at saturating $[Ca^{2+}]$ and at zero $[Ca^{2+}]$, respectively. The Ca^{2+} titration values fitted the Hill equation, $y=(y_{max} \cdot [Ca^{2+}]^n) / (K^n + [Ca^{2+}]^n)$, where y is $(R-R_{min}) / (R_{max}-R_{min})$, K is the dissociation constant, K_d, and n is the Hill coefficient. The effects of pH were monitored with GAP2 using different buffers for each pH range: histidine for pH 5.5 to 6.5, MOPS/Na for pH range 6.5-7.5 and Tris/HCl for pH 8-8.5. The effects of Mg^{2+} were monitored by varying the added $MgCl_2$ between 0.1 and 5 mM.

Cell culture and expression in mammalian cells

HeLa cells were maintained in Dulbecco's Modified Eagle Medium (DMEM) (Invitrogen) supplemented with 10% fetal bovine serum, 2 mM L-glutamine, 100 µg/ml streptomycin and 100 U/ml penicillin. Stable HeLa clones expressing erGAP2 or erGAP3 were obtained by lipofectamine transfection followed by G-418 selection. The population of GFP positive cells was enriched by cell sorting. Single-cell clones were selected in culture medium containing 0.8 mg/ml G-418 by limited dilution and maintained in 0.1 mg/ml G-418. For imaging experiments, 5 x 10^4 cells were seeded on poly-L-lysine coated 12 mm-diameter coverslips.

Cortical astrocyte cultures

Brain cortices were dissected from three P2-3 C57BL/6JCrl (Charles Rivers) mice in cold HBSS and digested with 0.5 mg/ml papain and 0.04 mg/ml DNase dissolved in a Ca^{2+}- and Mg^{2+}-free HBSS with 10 mM glucose and 0.1% bovine serum albumin (BSA) at 37ºC for 20 min. The cells were resuspended with Minimal Essential Medium (MEM) supplemented with 2 mM glutamax, 27 mM glucose, 100 µg/ml streptomycin, 100 U/ml penicillin and 10% (v/v) horse serum, and plated on a poly-L-lysine coated 75 cm^2 flask. After 2 and 7 days flasks were slapped to remove neurons and other loosely attached cells such as microglia and oligodendrocytes. After one week, cells were trypsinized and seeded in the same medium onto poly-L-lysine coated 12 mm-diameter glass coverslips at a density of 2.5 x 10^4 cells/coverslip. The cultures were used within 1-2 weeks.

Virus production

Packaging and titration of Herpes Simplex Virus 1 (HSV1) vectors were performed as reported earlier (Alonso, et al., 1998). Astrocyte cultures were infected with a multiplicity of infection (moi) ranging between 0.01 and 0.1 one day before use.

Ca^{2+} imaging

HeLa cell imaging was performed in a Nikon Diaphot inverted microscope using a 20x PlanApoUV objective (NA =0.7, Olympus) as described previously (Villalobos, et al., 1997). Briefly, standard medium containing 145 mM NaCl, 5 mM KCl, 1 mM $CaCl_2$, 1 mM $MgCl_2$, 10 mM glucose, 10 mM Na–HEPES, pH 7.4, were applied at 22-25ºC by perfusion at 5-6 ml/min. GAP was excited using the two filters, 403/12 DF and 470/25 DF, and a DM500 dichroic mirror. Cells were alternately epi-illuminated at 403 and 470 nm and light emitted above 520 nm was recorded using a Hamamatsu C4742-98 camera handled by the Simple PCI 6.6 Hamamatsu software. For simultaneous recording of $[Ca^{2+}]_{ER}$ and $[Ca^{2+}]_C$, erGAP-expressing cells were incubated for 60 min with rhod-3 AM (2 μM, Molecular Probes) at 22 ºC (Fig. 1d). Cells were imaged in a Zeiss axioplan upright microscope equipped with a 20x objective (W-Achroplan, Zeiss; NA= 0.5), sequentially excited at 405, 470 and 540 nm, and fluorescence was read at >515 (535DF35) nm and >590 (LP590) nm. Output images were background-subtracted and ratioed pixel-to-pixel using ImageJ software. The ratio F_{470}/F_{403} was used as an index of $[Ca^{2+}]_{ER}$ and F_{540}, generally expressed as F/F_0, as an index of $[Ca^{2+}]_C$. F_0 was the average of the fluorescence values obtained during the first 5-10 frames. $[Ca^{2+}]_C$ was also measured using fura-2 (Fig. S2b) as described previously (Rodriguez-Garcia, et al., 2014). Astrocyte imaging was performed similarly.

Generation of transgenic mice

The 5 kb transgene (Fig. S3a) containing either the erGAP2 or the erGAP3 gene was injected into C57BL/6JCrl (Charles Rivers) or B6CBAF2/OlaHsd (Harlan) oocytes, respectively, using standard techniques. Genotyping was routinely performed by PCR of genomic DNA obtained from tail biopsies using 4 oligonucleotides No. 30 and 31 of Table S3 for GAP (234 bp product), together with No. 32 and 33 for endogenous glyceraldehyde 3-phosphate dehydrogenase (GAPDH), a housekeeping gene (350 bp product). Experiments shown here were performed with mice of line 3 for erGAP2 and lines 1 and 10 for erGAP3. Experiments conformed to the institutional and national regulatory standards concerning animal welfare.

Calcium imaging in brain slices

Acute hippocampal slices were prepared from mice (P7-P15) from transgenic lines erGAP2 (L3) or erGAP3 (L1 or L10). The hippocampus was dissected out along with the cortex and sliced into 350-400µm thick sections with a McIlwain Tissue Chopper. Slices were quickly transferred to a fine-meshed membrane filter and maintained in artificial cerebrospinal fluid (ACSF) containing: 125 mM NaCl, 2.5 mM KCl, 1 mM $MgCl_2$, 26 mM $NaHCO_3$, 1 mM $CaCl_2$, 10 mM glucose, 1.25 mM NaH_2PO_4, pH7.4, continuously bubbled with a 95% O_2 / 5% CO_2 gas mixture at 25ºC. Slices were mounted onto the stage of a Zeiss Axioplan upright microscope equipped with a 5x objective (Plan-Neofluar, Zeiss; NA= 0.15) and a Zeiss AxioCam camera MRm (12 bit) connected through a software interface (Axiovision, Zeiss) to a Xenon fluorescent excitation source and a filter wheel. GAPs were excited at 405 and 470 nm and acquired at 518-553 nm, as described above. For simultaneous measuring of $[Ca^{2+}]_{ER}$ and $[Ca^{2+}]_C$, slices were incubated for 1 h at room temperature with 16 µM rhod-3 AM in bubbled ACSF medium. Imaging was performed as

described above for HeLa cells. All the experiments were performed at 22-25ºC in a custom-made chamber of 42 µl volume under constant perfusion at 3 ml/min.

Generation of transgenic flies

PhiC31 system-mediated (Bischof, et al., 2007) transformation of *Drosophila melanogaster* strain "y^1 M{vas-int.Dm}ZH-2A w*; M{3xP3-RFP.attP} ZH-86Fb" (BL24749) was used. pUASTattB-erGAP3 was injected into embryos and stable lines with the transgene incorporated into an *attP86* site on the third chromosome were selected (BestGene Inc, USA). We used the Gal4-UAS system (Brand and Perrimon, 1993) to express erGAP3 in muscle cells. UAS-erGAP3 or UAS-GCaMP3 flies (Tian, et al., 2009) were crossed with myosin heavy chain (*Mhc*)-Gal4 flies (Schuster, et al., 1996).

Calcium imaging in flies

Adult *Drosophila* were anesthetized with CO_2, tethered ventrally with a small drop of agar and then gently transferred to the microscope stage. Recordings of the dorsal longitudinal muscles (DLM) in the fly thorax were obtained by stimulation of the giant fiber system through two tungsten electrodes impaled into the fly eyes (Allen and Godenschwege, 2010). The stimulation protocol consisted of voltage stimuli of 5-10 V and 30-50 ms duration at different frequencies (0.25 to 16 Hz). Each experiment started with a visual check of twitches in the wing after stimulation. Fluorescence images were acquired with a Leica MZ16FA Fluorescence Stereo Microscope equipped with a Plan Apo 1.0x objective (N.A., 0.14) and a 100W mercury lamp, using either 470/40 nm or 405/40 excitation filters and a 525/50 nm emission filter. Images were acquired at 12 bits with binning of 2x2 or 4x4 and a zoom of 6.5x.

Statistical analysis

Results are expressed as mean ± SD or mean±SEM, as indicated. The statistical significance was evaluated using Student's t-test or one-way ANOVA with GraphPad InStat3 software.

ACKNOWLEDGMENTS

We thank M. García Cubillas for technical assistance; I. López , Y. Gaciño and F. Martínez for assistance with mice; A. Martín for assistance in cell sorting; J. Fernández, C. Lázaro and R. Pascua-Maestro for help with flies; and M. Torres and L.M. Criado for mouse microinjections. We thank A. Ferrús (Instituto Cajal, Madrid, Spain) for providing *Mhc*-Gal4 flies. Preliminary recordings in *Drosophila* were performed by the medical student J. González Zamora. This work was supported by grants from the Spanish Ministerio de Economia y Competitividad (BFU2014-53469P), and the Instituto de Salud Carlos III (TerCel; RD12/0019/0036)

AUTHOR CONTRIBUTIONS

J.G.-S. and M.T.A. conceived and designed the study. M.T.A. was responsible for molecular biology designs. L.L.L. helped with the design of the low affinity mutations for Ca^{2+}. M.D.G. helped with the design and execution of the experiments in flies. P.N.-N- and J.R.-R. and M.R.-P. performed the experiments and analyzed the data. J.G.-S- and M.T.A. wrote the manuscript. J.G.-S. supervised the whole study. All authors discussed the conceptual and practical implications of the results.

COMPETING FINANCIAL INTERESTS

The authors declare no competing financial interests.

REFERENCES

1. Alonso, M.T., Barrero, M.J., Carnicero, E., Montero, M., Garcia-Sancho, J., and Alvarez, J. (1998). Functional measurements of [Ca2+] in the endoplasmic reticulum using a herpes virus to deliver targeted aequorin. Cell Calcium 24, 87-96.
2. Alonso, M.T., Barrero, M.J., Michelena, P., Carnicero, E., Cuchillo, I., Garcia, A.G., Garcia-Sancho, J., Montero, M., and Alvarez, J. (1999). Ca2+-induced Ca2+ release in chromaffin cells seen from inside the ER with targeted aequorin. J Cell Biol 144, 241-254.
3. Allen, M.J., and Godenschwege, T.A. (2010). Electrophysiological recordings from the Drosophila giant fiber system (GFS). Cold Spring Harb Protoc 2010, pdb prot5453.
4. Aulestia, F.J., Alonso, M.T., and Garcia-Sancho, J. (2015). Differential calcium handling by the cis and trans regions of the Golgi apparatus. Biochem J 466, 455-465.
5. Bischof, J., Maeda, R.K., Hediger, M., Karch, F., and Basler, K. (2007). An optimized transgenesis system for Drosophila using germ-line-specific phiC31 integrases. Proc Natl Acad Sci U S A 104, 3312-3317.
6. Brand, A.H., and Perrimon, N. (1993). Targeted gene expression as a means of altering cell fates and generating dominant phenotypes. Development 118, 401-415.
7. Dallwig, R., Vitten, H., and Deitmer, J.W. (2000). A novel barium-sensitive calcium influx into rat astrocytes at low external potassium. Cell Calcium 28, 247-259.
8. Fernandez-Santiago, R., and Ezquerra, M. (2016). Epigenetic Research of Neurodegenerative Disorders Using Patient iPSC-Based Models. Stem Cells Int 2016, 9464591.
9. Fernandez de Sevilla, D., Nunez, A., Borde, M., Malinow, R., and Buno, W. (2008). Cholinergic-mediated IP3-receptor activation induces long-lasting synaptic enhancement in CA1 pyramidal neurons. J Neurosci 28, 1469-1478.
10. Gallego-Sandin, S., Alonso, M.T., and Garcia-Sancho, J. (2011). Calcium homoeostasis modulator 1 (CALHM1) reduces the calcium content of the endoplasmic reticulum (ER) and triggers ER stress. Biochem J 437, 469-475.

11. Henderson, M.J., Baldwin, H.A., Werley, C.A., Boccardo, S., Whitaker, L.R., Yan, X., Holt, G.T., Schreiter, E.R., Looger, L.L., Cohen, A.E., et al. (2015). A Low Affinity GCaMP3 Variant (GCaMPer) for Imaging the Endoplasmic Reticulum Calcium Store. PLoS One 10, e0139273.
12. Kienzle, C., and von Blume, J. (2014). Secretory cargo sorting at the trans-Golgi network. Trends Cell Biol 24, 584-593.
13. Miyazaki, J., Takaki, S., Araki, K., Tashiro, F., Tominaga, A., Takatsu, K., and Yamamura, K. (1989). Expression vector system based on the chicken beta-actin promoter directs efficient production of interleukin-5. Gene 79, 269-277.
14. Moore, G.A., Kass, G.E., Duddy, S.K., Farrell, G.C., Llopis, J., and Orrenius, S. (1990). 2,5-Di(tert-butyl)-1,4-benzohydroquinone--a novel mobilizer of the inositol 1,4,5-trisphosphate-sensitive Ca2+ pool. Free Radic Res Commun 8, 337-345.
15. Palmer, A.E., and Tsien, R.Y. (2006). Measuring calcium signaling using genetically targetable fluorescent indicators. Nat Protoc 1, 1057-1065.
16. Power, J.M., and Sah, P. (2002). Nuclear calcium signaling evoked by cholinergic stimulation in hippocampal CA1 pyramidal neurons. J Neurosci 22, 3454-3462.
17. Rodriguez-Garcia, A., Rojo-Ruiz, J., Navas-Navarro, P., Aulestia, F.J., Gallego-Sandin, S., Garcia-Sancho, J., and Alonso, M.T. (2014). GAP, an aequorin-based fluorescent indicator for imaging Ca2+ in organelles. Proc Natl Acad Sci U S A 111, 2584-2589.
18. Schuster, C.M., Davis, G.W., Fetter, R.D., and Goodman, C.S. (1996). Genetic dissection of structural and functional components of synaptic plasticity. I. Fasciclin II controls synaptic stabilization and growth. Neuron 17, 641-654.
19. Suzuki, J., Kanemaru, K., Ishii, K., Ohkura, M., Okubo, Y., and Iino, M. (2014). Imaging intraorganellar Ca2+ at subcellular resolution using CEPIA. Nat Commun 5, 4153.
20. Tang, S., Wong, H.C., Wang, Z.M., Huang, Y., Zou, J., Zhuo, Y., Pennati, A., Gadda, G., Delbono, O., and Yang, J.J. (2011). Design and application of a class of sensors to monitor Ca2+ dynamics in high Ca2+ concentration cellular compartments. Proc Natl Acad Sci U S A.

21. Thastrup, O., Dawson, A.P., Scharff, O., Foder, B., Cullen, P.J., Drobak, B.K., Bjerrum, P.J., Christensen, S.B., and Hanley, M.R. (1989). Thapsigargin, a novel molecular probe for studying intracellular calcium release and storage. Agents Actions 27, 17-23.
22. Tian, L., Hires, S.A., Mao, T., Huber, D., Chiappe, M.E., Chalasani, S.H., Petreanu, L., Akerboom, J., McKinney, S.A., Schreiter, E.R., et al. (2009). Imaging neural activity in worms, flies and mice with improved GCaMP calcium indicators. Nat Methods 6, 875-881.
23. Verkhratsky, A., Rodriguez, J.J., and Parpura, V. (2012). Calcium signalling in astroglia. Mol Cell Endocrinol 353, 45-56.
24. Villalobos, C., Nunez, L., Frawley, L.S., Garcia-Sancho, J., and Sanchez, A. (1997). Multi-responsiveness of single anterior pituitary cells to hypothalamic-releasing hormones: a cellular basis for paradoxical secretion. Proc Natl Acad Sci U S A 94, 14132-14137.
25. Wan, W., Cao, L., Kalionis, B., Xia, S., and Tai, X. (2015). Applications of Induced Pluripotent Stem Cells in Studying the Neurodegenerative Diseases. Stem Cells Int 2015, 382530.
26. Wu, J., Prole, D.L., Shen, Y., Lin, Z., Gnanasekaran, A., Liu, Y., Chen, L., Zhou, H., Chen, S.R., Usachev, Y.M., et al. (2014). Red fluorescent genetically encoded Ca2+ indicators for use in mitochondria and endoplasmic reticulum. Biochem J 464, 13-22.

FIGURE LEGENDS

Figure 1. Characterization of the new GAP sensors. (a) ER Ca^{2+} emptying monitored with erGAP in HeLa cells. Comparison of the GAP1 and GAP2 submaximal responses to stimulation with ATP + carbachol (labelled as ATP; 100 µM each) followed by full ER emptying by stimulation with the same stimuli applied in Ca^{2+}-free medium containing 10 µM of the SERCA inhibitor TBH. Traces are the average of 14 (GAP1) or 20 (GAP2) cells. Experiments were performed in cell lines stably expressing erGAP1 or erGAP2. **(b)** Purified-protein Ca^{2+} titrations of GAP2 and GAP3; curves fit with Hill equation $y = (y_{max} \cdot [Ca^{2+}]^n) / (K_d^n + [Ca^{2+}]^n)$, yielding (mean±SEM; n=3): GAP2 K_d = 407 ± 37 and n=1.0 ± 0.1; GAP3, K_d =489 ± 43 µM and n =0.9 ± 0.1. For more details see Fig. S1. **(c)** Response of erGAP3-expressing HeLa cells to repeated stimulation with ATP + carbachol (details as in **a**) followed by response in Ca^{2+}-free medium containing 10 µM TBH; CAF stands for 50 mM caffeine. Trace is the average of 34 cells. Note the reciprocal changes of the individual fluorescence channels, F470 and F405. (**d**) F470/F405 ratio (R) normalized to R_0 (R/R_0) was shown alongside simultaneous measurement of cytosolic Ca^{2+} with Rhod-3 (F/F_0).

Figure 2. Use of erGAP for monitoring ER-Ca^{2+} oscillations in cultured astrocytes. (a) Oscillations of $[Ca^{2+}]_{ER}$ induced by low K^+ (0.2 mM) in erGAP2–expressing astrocytes. The upper row shows a gray-scale GAP fluorescence image in which 4 nuclei (n1-n4) can be seen. Next to it, the contours of the four cells and the pseudocolored ratio image at baseline (REST) and at maximum response with ATP (+ATP; 100 µM) are shown. The pseudocolor scale and the trace of cell 2 are shown at right. Video 1 shows the whole experiment. The lower row shows a series

of 9 images taken during one of the oscillations at a frame rate of 1 image every 10 s. Note that the $[Ca^{2+}]_{ER}$ drop starts in cell 1 (frame 1; start at the arrowhead), progresses towards cell 2 (frame 2; arrowhead), invades it (frames 3 and 4) and, finally reaches cell 3 (frames 5 and 6). At frame 7, refilling of the ER calcium stores begins (at the arrowhead). Note that cell 4 oscillates independently. It is maximally depleted at frame 1 and refills during frames 2-9. **(b)** Synchronization of ER Ca^{2+} release during Ca^{2+} oscillations in astrocytes. The same experiment as in **a** is shown. Regions of interest (1-7) were defined in different cells as shown over the pseudocolored image, which is the average of all the images of the whole experiment. Ordinate: R/R_0 in arbitrary units. Traces have been displaced vertically for better visibility. AVG, averaged value of the 7 cells in the field. Note that $[Ca^{2+}]_{ER}$ decrease (D) is synchronous at D1 (D, ATP-induced), whereas D2-D5 start in one cell and then progress to the others.

Figure 3. Functional mapping of acetylcholine responses in hippocampal slices *ex vivo*. (a) Frame sequence during stimulation with acetylcholine (ACh; 200 μM, 30 s) in acute hippocampal slices from erGAP3 transgenic mice (line 10; P7). Cornus ammonis regions (CA) and the upper blade of dentate gyrus (DG) are visible. Measurements of ER- (erGAP3) and cytosolic (Rhod-3) Ca^{2+} were performed simultaneously. Frames were acquired every 10 s. Upper row: ER Ca^{2+} release, evidenced by the decrease of the GAP signal in CA1, during ACh stimulation. Calibration bar, 200 μm. Lower row, coordinated increase of Rhod-3 fluorescence, indicating the increase of $[Ca^{2+}]_C$ by release from the ER. **(b)** Detailed kinetics of experiment shown in **a**. Each graph symbol corresponds to 10 s. Note that the peak increase of $[Ca^{2+}]_C$ occurs 10 s after the application of ACh, whereas maximum

$[Ca^{2+}]_{ER}$ decrease required more than 30 s. The relaxation of the $[Ca^{2+}]_C$ peak was also faster than the one of the $[Ca^{2+}]_{ER}$ peak. Video 2 shows the changes in erGAP3 during the whole experiment. Similar results were obtained with erGAP2 transgenic mice (line 3).

Figure 4. Monitoring $[Ca^{2+}]_{ER}$ dynamics during muscle contraction in the living fly with erGAP3. (a, b) Specific expression of erGAP3 (green fluorescence) in the thoracic muscle of *Mhc*-erGAP3 fly. Lateral view of bright field and fluorescence image were superimposed in **(a).** Dorsal view of fluorescence and the ROI where it was quantified is shown in **(b).** The muscles were stimulated via the giant fiber (see Methods) at different frequencies with 5-10 V / 30-50 ms stimuli. **(c)** Individual SR release Ca^{2+} events seen during stimulation at low frequency (0.5 Hz). Reciprocal responses of the GAP3 fluorescence excited at 470 and 405 nm. Fluorescence images were acquired every 100 ms. **(d)** Comparison of ER Ca^{2+} release during stimulation at low- (0.25 Hz) and high-frequency (4 and 16 Hz). The traces of fluorescence excited at 470 nm are shown. **(e)** Complementary changes in the cytosolic Ca^{2+} (F/F_0), measured with GCaMP3.

Supplementary Information

Figure S1. Sensitivity of GAP2 to Mg^{2+} and pH.

Figure S2. Calibration of erGAP in single HeLa cells.

Figure S3. Generation of erGAP transgenic mice and expression in the hippocampus.

Figure S4. Frequency-dependent summation of elementary muscle SR Ca^{2+} release events during repetitive neural stimulation of living flies.

Movie S1. $[Ca^{2+}]_{ER}$ oscillations in astrocytes.

Movie S2. Neurotransmitter functional mapping in hippocampal slices.

Table S1. Screening for low Ca^{2+} affinity GAP mutants.

Table S2. Re-engineering of the GFP moiety to increase GAP fluorescence.

Table S3. Oligonucleotides used for mutagenesis and genotyping of transgenic mice.

Supplementary References

Supplementary Figure Legends

Fig. S1. Sensitivity of GAP2 to Mg^{2+} and H^{+}. **(a)** Sensitivity to Mg^{2+}; measurements were performed in solution containing 140 mM KCl, 0.1, 1 or 5 mM $MgCl_2$ and 20 mM MOPS/Na, pH 7.2. (**b)** Sensitivity to pH; measurements performed in solution containing 140 mM KCl, 1 mM $MgCl_2$ and the following buffers (20 mM): pH 5.5-6.0, histidine/HCl; pH 6.5-7.5, MOPS/Na; pH 8.5, Tris/HCl. At pH 6 or below the Ca^{2+} affinity was substantially decreased.

Fig. S2. Calibration of erGAP in single HeLa cells. The erGAP2 stably expressing clone was used. The trace is the average of 37 cells. Values were normalized to R_0 or F_0. **(a)** Cells were perfused with standard incubation medium containing either 1 mM Ca^{2+} or no Ca^{2+} (0.1 mM EGTA) and 100 μM ATP or 200 nM thapsigargin as shown. **(b)** Details as in **a**, except that cells were first loaded with Fura-2 by incubation with 2 μM Fura-2/AM for 90 min. GAP2 fluorescence was measured only at 470 nm excitation and it is expressed as F/F_0. Fura-2 fluorescence was measured at 340 and 380 nm excitation and is expressed as the ratio of the two fluorescences. TBH, 10 μM tert-butylhydroquinone; 5 Ca, standard medium containing 5 mM Ca^{2+}.

Fig. S3. Generation of erGAP transgenic mice and expression in the hippocampus. **(a)** The transgene construct included the following elements: CMV, cytomegalovirus early enhancer; cβA, chicken β-actin 5'-UTR; CAGp, promoter; I1, intron 1 (first intron of chicken β-actin gene); K, Kozac sequence; CR, human calreticulin signal peptide (MLLSVPLLLGLLGLAVAND); GAP2/GAP3, GFP-Aequorin Protein 2 or 3; KDEL, ER-retention tag; I2, intron 2; WPRE, woodchuck virus post-transcriptional regulatory element; polyA, bovine growth hormone polyadenylation sequence; βG polyA, β-globin polyadenylation sequence. Restriction enzyme sites for excision of the transgene are indicated (arrows). **(b)** Fluorescent image of a live hippocampus slice (350 μm thickness) isolated from erGAP3 transgenic mice (Line 1; P5) taken at 470 nm excitation during 450 ms.

Fig. S4. Frequency-dependent summation of elementary muscle SR Ca^{2+} release events during repetitive neural stimulation of living flies. The values of F/F0 for the fluorescences excited at 470 nm are shown. The decreases of the signal obtained at different stimulation frequencies are compared: 0.2 Hz **(a)**, 4 Hz **(b)**, and 16 Hz **(c)**. Other details as in **Fig. 4d**. Images were taken at a rate of 1 frame every 100 ms.

Supplementary Movies:

Video S1. $[Ca^{2+}]_{ER}$ oscillations in astrocytes. Cultured astrocytes expressing erGAP2 were first stimulated with a maximal ATP challenge during 1 min ER refilled rapidly upon stimulus washout. Then, cells were perfused with low-K^{+} (0.2 mM) medium for 5 min to induce Ca^{2+} entry; this resulted in $[Ca^{2+}]_{ER}$ oscillations. On return to control medium containing 5 mM K^{+} the oscillations disappeared and ER refilled quickly with Ca^{2+} recovering the baseline values.

Video S2. Neurotransmitter functional mapping in hippocampal slices. The slices were stimulated with ACh (200 μM) for 30 s and then returned to control solution. Simultaneous measurements of $[Ca^{2+}]_{ER}$ (GAP3) and $[Ca^{2+}]_C$ (Rhod-3) are shown.

Table S1. Screening for low Ca^{2+} affinity GAP mutants. The fluorescence was measured as described in Methods (GAP screening section). The low affinity mutants should give values larger than 1 in the last column. The lowest affinity mutant was No. 2, and was named GAP2.

		R_{Ca} / R_{EGTA}		RATIO
No.	**Mutated residues**	**0.1 mM Ca^{2+}**	**1 mM Ca^{2+}**	**1 mM / 0.1 mM**
1	(D24H,D119A)	1.019	1.040	1.02
2	(D24N,D119A)	1.180	2.084	1.77
3	(D24V,D119A)	2.527	2.604	1.03
4	(V25P,D119A)	3.314	3.214	0.97
5	(N28Q,D119A)	1.002	1.046	1.04
6	(N28V,D119A)	0.998	1.014	1.02
7	(D35Q,D119A)	2.199	2.411	1.10
8	(Y38S,D119A)	2.405	2.289	0.95
9	(D117N,D119A)	0.998	1.022	1.03
10	(D117V,D119A)	2.393	2.423	1.01
11	(D119K)	2.057	2.270	1.10
12	(D119I)	1.426	1.506	1.06
13	(D119A,N121L)	2.933	3.366	1.15
14	(D119A,E128K)	2.509	2.610	1.04
15	(D119A,E128R)	2.626	2.913	1.11
16	(D119A,D153L)	2.373	2.345	0.99
17	(D119A,D155K)	2.260	2.442	1.08
18	(D119A,E156N)	2.485	2.549	1.03
19	(D119A,E156P)	0.981	0.942	0.96
20	(D119A,S157Q)	1.985	2.553	1.29
21	(D119A,D161K)	1.072	1.112	1.05
22	(D119A,E164K)	2.235	2.434	1.10

Table S2. Re-engineering of the GFP moiety to increase GAP fluorescence. GAP2 was humanized for codon usage and re-engineered in different residues of the GFP moiety to increase GAP fluorescence (Heim, et al., 1994; Tallini, et al., 2006; Tian, et al., 2009; Zacharias, et al., 2002; Zhao, et al., 2011). In 6 variants the Ca^{2+}-sensitivity was lost. Mutant No. 7, named GAP3, gave the maximum increase in fluorescence

Mutant No.	**MUTATION**						**Ca^{2+} sensitive**
	S175G	**D180Y**	**I167V**	**L15Q**	**A206I**	**T153K**	
1	X	X		X	X		No
2	X	X	X	X	X	X	No
3	X	X	X	X	X		No
4	X	X	X	X	X	X	No
5	X	X	X	X		X	Yes
6	X	X	X		X		No
7	X	X	X	X			Yes
8			X	X	X		No

Table S3. Oligonucleotides used for mutagenesis and genotyping of transgenic mice.

No.	Mutation	Sequence
1	D24H	GTTCAATTTCCTTCATGTCAACCACAATGG
2	D24N	GTTCAATTTCCTTAATGTCAACCACAATGG
3	D24V	GTTCAATTTCCTTGTTGTCAACCACAATGG
4	D25P	AATTTCCTTGATCCCAACCACAATGG
5	N28Q	TGTCAACCACCAAGGAAAAATCTC
6	N28V	TGTCAACCACGTCGGAAAAATCTC
7	E35Q	GGAAAAATCTCTCTTGACCAGATGGTCTACAAGGCATC
8	Y38S	ACGAGATGGTCTCCAAGGCATCTG
9	D117N	GTTTGACATCGTTAACAAAGCCCAAAATGG
10	D117V	GCTTTGTTTGACATCGTTGTCAAAGCCCAAAATGGAGC
11	D119K	ATCGTTGACAAAAAGCAAAATGGAGC
12	D119I	ATCGTTGACAAAATTCAAAATGGAGC
13	N121L	TGACAAAGCCCAACTTGGAGCTATTACAC
14	E128K	ATTACACTGGATAAATGGAAAGCATAC
15	E128R	ATTACACTGGATAGATGGAAAGCATAC
16	D153L	GAAACATTCAGAGTGTGCCTTATTGATGAAAGTGGACAACTCG
17	D155K	TTCAGAGTGTGCGATATTAAAGAAAGTGGACAACTCG
18	E156N	TGCGATATTGATAATAGTGGACAACTC
19	E156P	TGCGATATTGATCCAAGTGGACAACTC
20	S157Q	ATATTGATGAACAAGGACAACTCGATG
21	D161K	AGTGGACAACTCAAAGTTGATGAGATG
22	E164K	CTCGATGTTGATAAGATGACAAGAC
23	D175G	CAACATAGAAGACGGCGGCGTACAGCTGGC
24	D180Y	AGAAGACGGCGGCGTACAGCTGGCTTACCACTATCAGC
25	I167V	AAAGCTAATTTCAAGGTGAGGCACAACATAGAAG
26	T153K	ATAATGTGTACATAAAGGCCGACAAACAGAAGAACG
27	L15Q	GTGGTCCCTATCCAGGTGGAACTCGATGG
28	A206I	TCTGTCCACACAATCAATCCTGAGCAAGGACCC
29	A206K	TCTGTCCACACAATCAAAGCTGAGCAAGGACCC
30	mGFPuv	GATGGCAACATCCTCGGACA
31	mGFPuv	GTCCTTGCTCAGGGCTGATT
32	hGAPDH	GTCTTCTGGGTGGCAGTGATGG
33	hGAPDH	CATCACCATCTTCCAGGAGCGA

Supplementary References

1. Heim, R., Prasher, D.C., and Tsien, R.Y. (1994). Wavelength mutations and posttranslational autoxidation of green fluorescent protein. Proc Natl Acad Sci U S A 91, 12501-12504.
2. Tallini, Y.N., Ohkura, M., Choi, B.R., Ji, G., Imoto, K., Doran, R., Lee, J., Plan, P., Wilson, J., Xin, H.B., et al. (2006). Imaging cellular signals in the heart in vivo: Cardiac expression of the high-signal Ca2+ indicator GCaMP2. Proc Natl Acad Sci U S A 103, 4753-4758.
3. Tian, L., Hires, S.A., Mao, T., Huber, D., Chiappe, M.E., Chalasani, S.H., Petreanu, L., Akerboom, J., McKinney, S.A., Schreiter, E.R., et al. (2009). Imaging neural activity in worms, flies and mice with improved GCaMP calcium indicators. Nat Methods 6, 875-881.
4. Zacharias, D.A., Violin, J.D., Newton, A.C., and Tsien, R.Y. (2002). Partitioning of lipid-modified monomeric GFPs into membrane microdomains of live cells. Science 296, 913-916.
5. Zhao, Y., Araki, S., Wu, J., Teramoto, T., Chang, Y.F., Nakano, M., Abdelfattah, A.S., Fujiwara, M., Ishihara, T., Nagai, T., et al. (2011). An expanded palette of genetically encoded Ca(2)(+) indicators. Science 333, 1888-1891.

Fig. 1

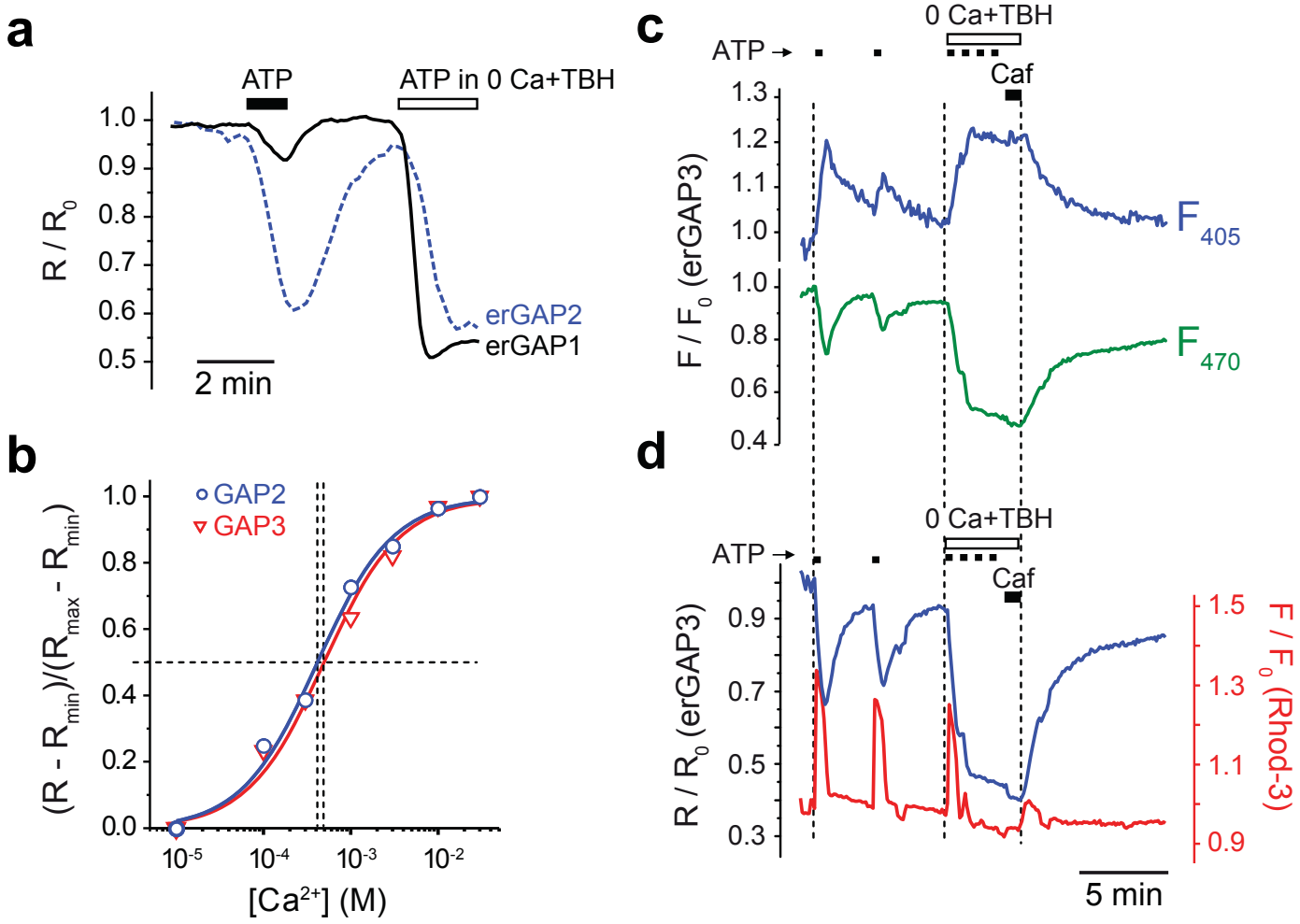
a
ATP
ATP in 0 Ca+TBH
R / R0
1.0
0.9
0.8
0.7
0.6
0.5
2 min
erGAP2
erGAP1
b
GAP2
GAP3
(R - Rmin)/(Rmax - Rmin)
1.0
0.8
0.6
0.4
0.2
0.0
10-5
10-4
10-3
10-2
[Ca2+] (M)
c
0 Ca+TBH
ATP
Caf
F / F0 (erGAP3)
1.3
1.2
1.1
1.0
1.0
0.8
0.6
0.4
F405
F470
d
0 Ca+TBH
ATP
Caf
R / R0 (erGAP3)
0.9
0.7
0.5
0.3
F / F0 (Rhod-3)
1.5
1.3
1.1
0.9
5 min

Fig. 2

a

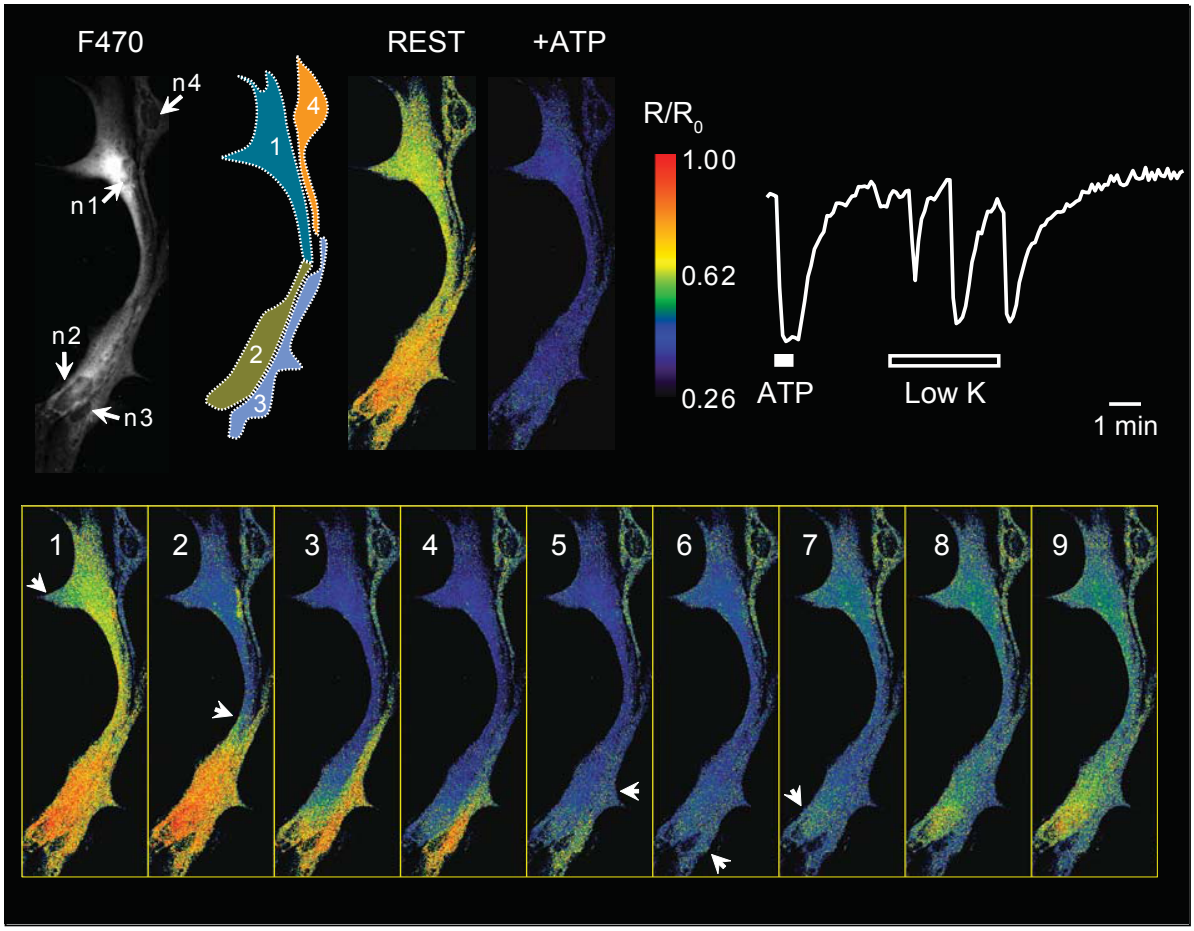
F470
REST
+ATP
n4
n1
n2
n3
1
2
3
4
R/R0
1.00
0.62
0.26
ATP
Low K
1 min
1
2
3
4
5
6
7
8
9

b

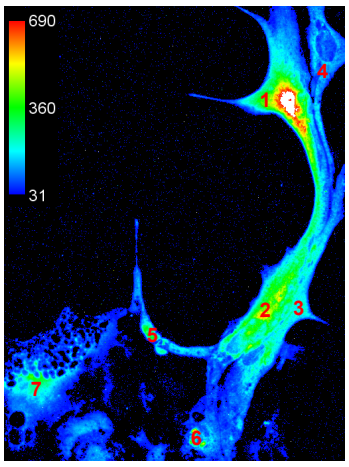
690
360
31
1
2
3
4
5
6
7

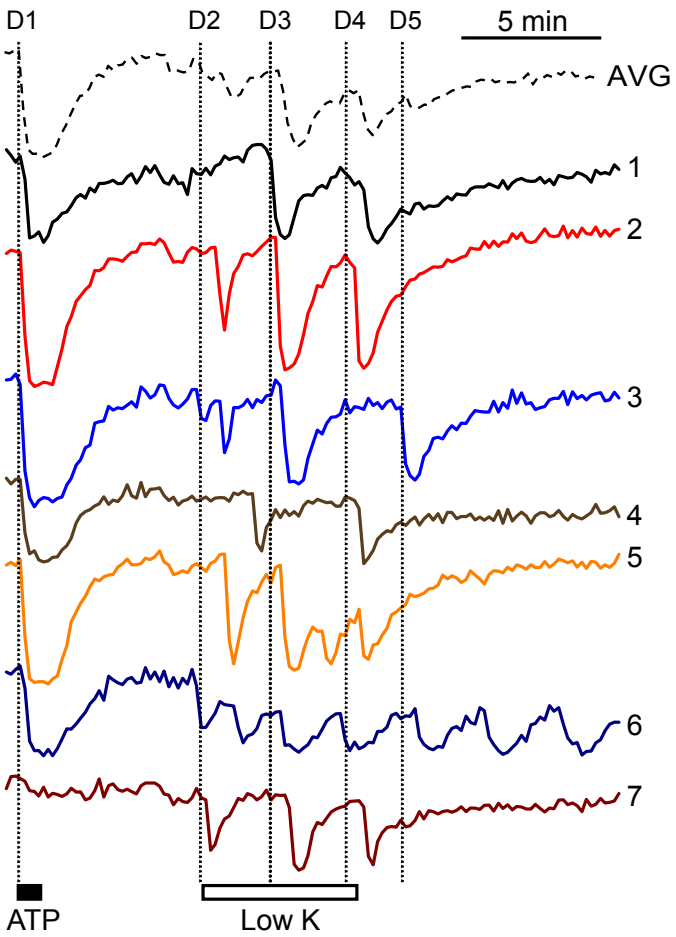
D1
D2
D3
D4
D5
5 min
AVG
1
2
3
4
5
6
7
ATP
Low K

Fig. 3

a

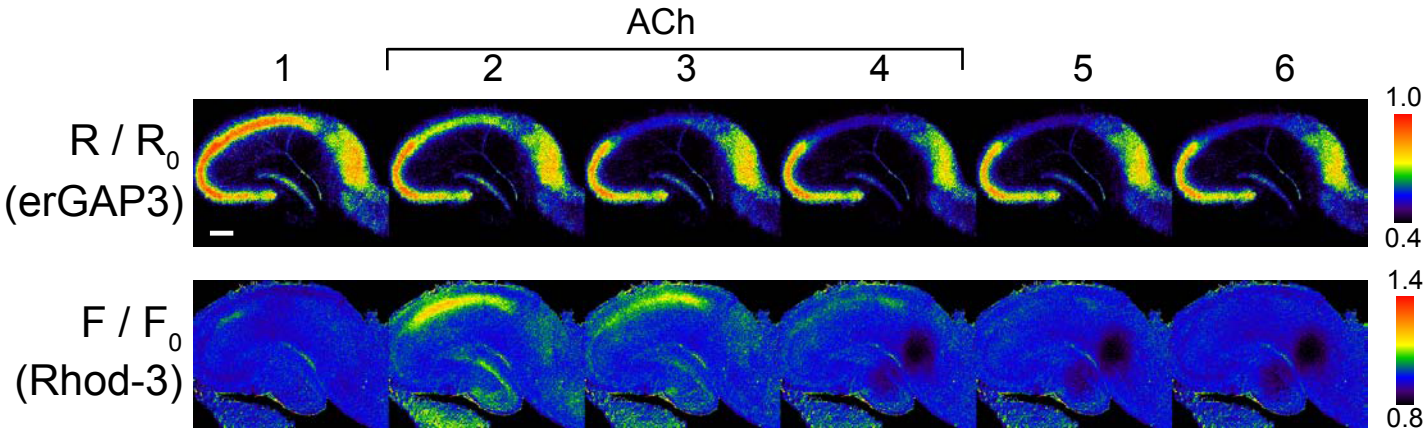
ACh
1
2
3
4
5
6
R / R0
(erGAP3)
1.0
0.4
F / F0
(Rhod-3)
1.4
0.8

b

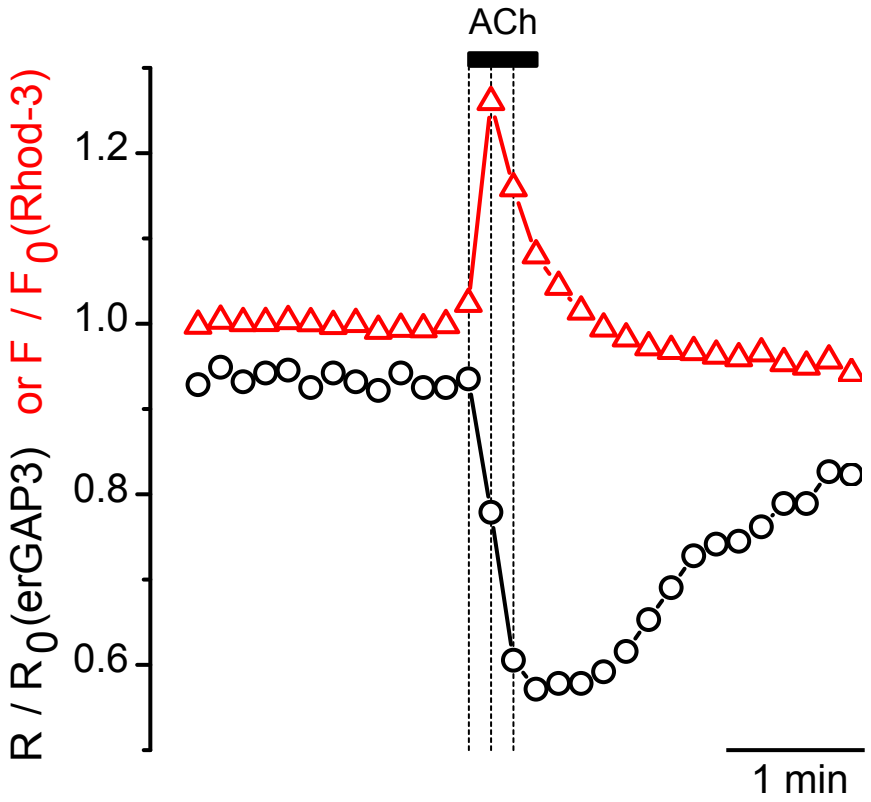
ACh
R / R0(erGAP3) or F / F0(Rhod-3)
1.2
1.0
0.8
0.6
1 min

Fig. 4

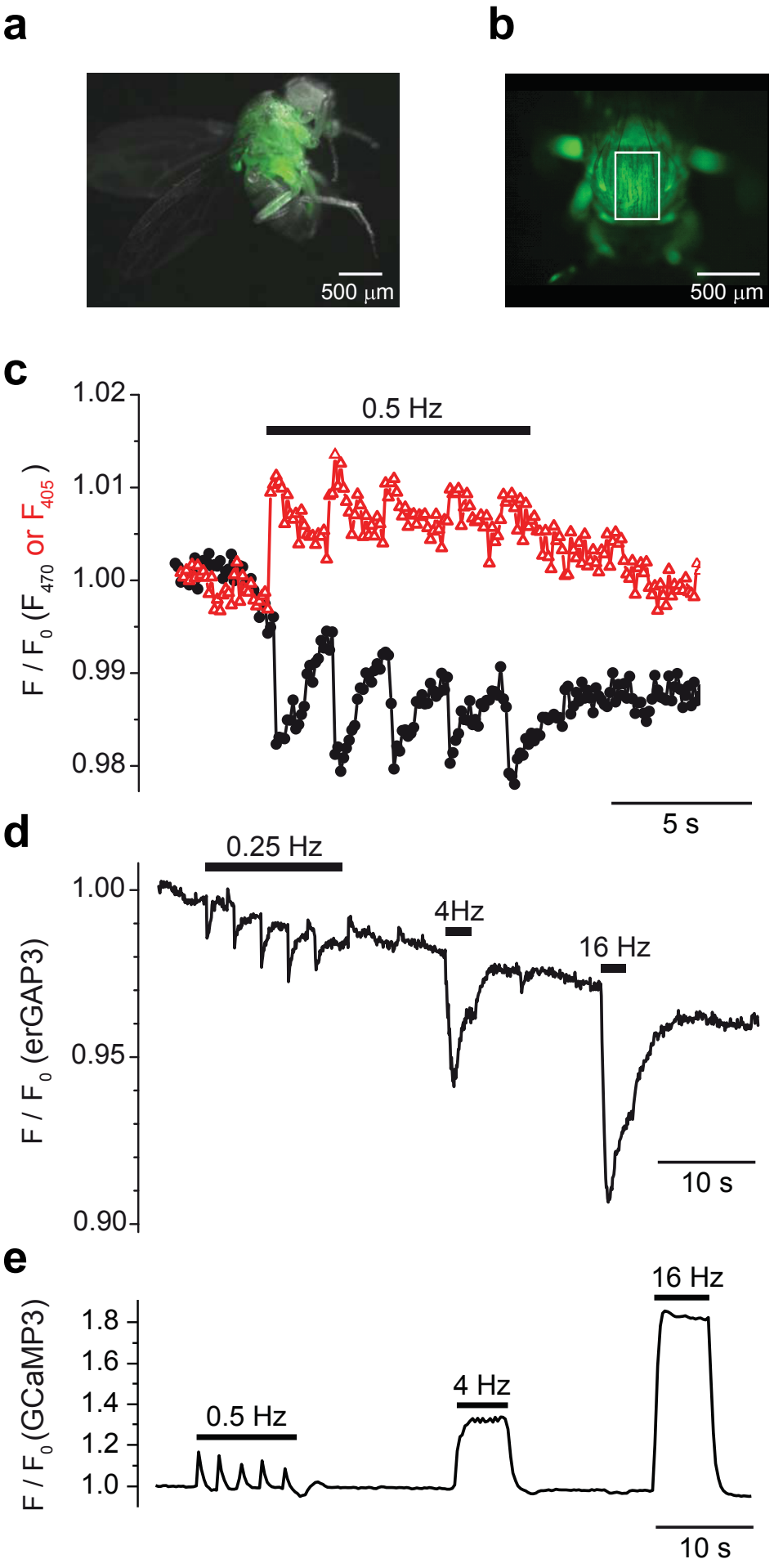
a
b
500 μm
500 μm
c
1.02
1.01
1.00
0.99
0.98
F / F0 (F470 or F405)
0.5 Hz
5 s
d
0.25 Hz
4Hz
16 Hz
1.00
0.95
0.90
F / F0 (erGAP3)
10 s
e
16 Hz
1.8
1.6
1.4
1.2
1.0
F / F0 (GCaMP3)
4 Hz
0.5 Hz
10 s

Fig. S1

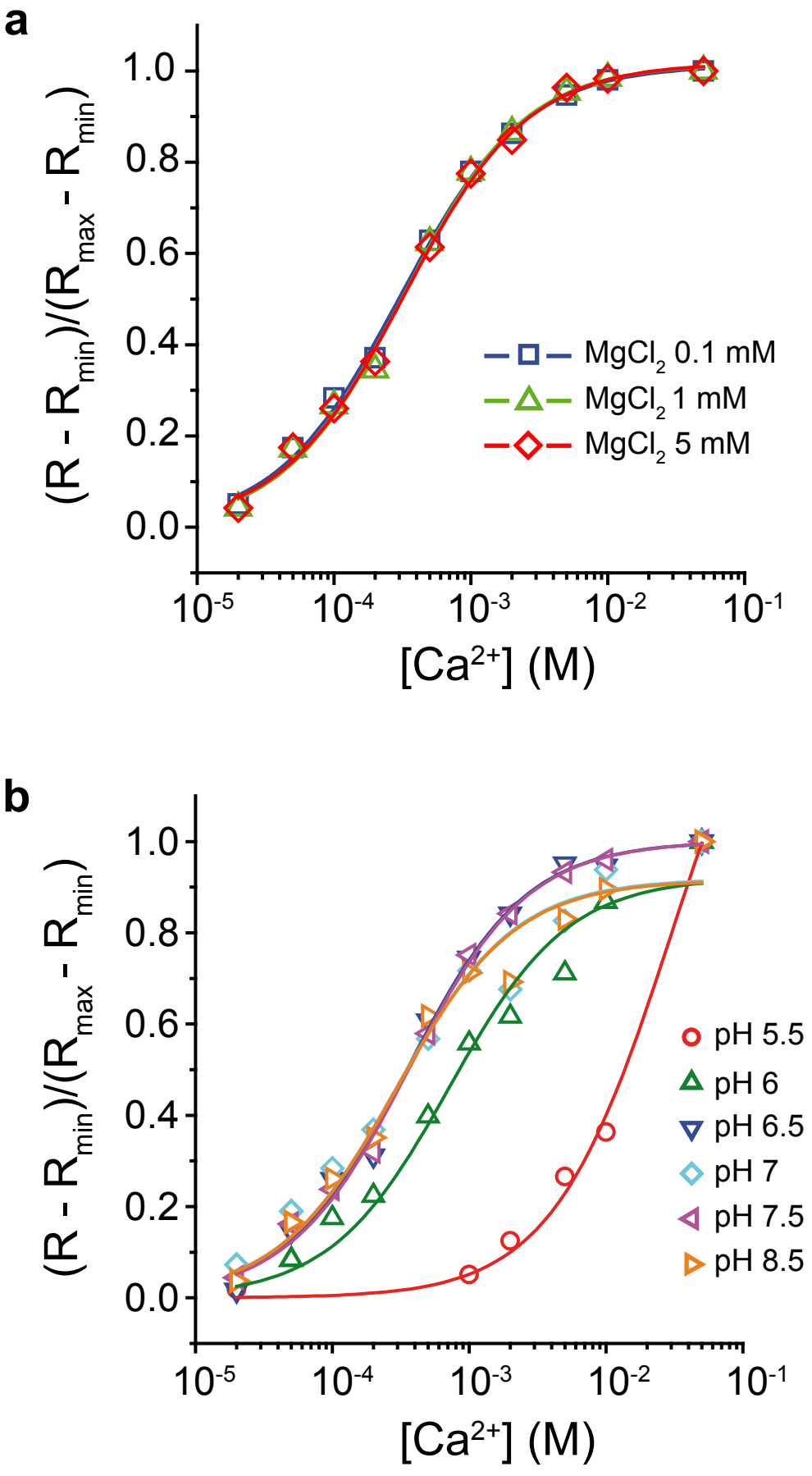
a
1.0
0.8
0.6
0.4
0.2
0.0
(R - Rmin)/(Rmax - Rmin)
MgCl2 0.1 mM
MgCl2 1 mM
MgCl2 5 mM
10-5
10-4
10-3
10-2
10-1
[Ca2+] (M)
b
1.0
0.8
0.6
0.4
0.2
0.0
(R - Rmin)/(Rmax - Rmin)
pH 5.5
pH 6
pH 6.5
pH 7
pH 7.5
pH 8.5
10-5
10-4
10-3
10-2
10-1
[Ca2+] (M)

Fig. S2

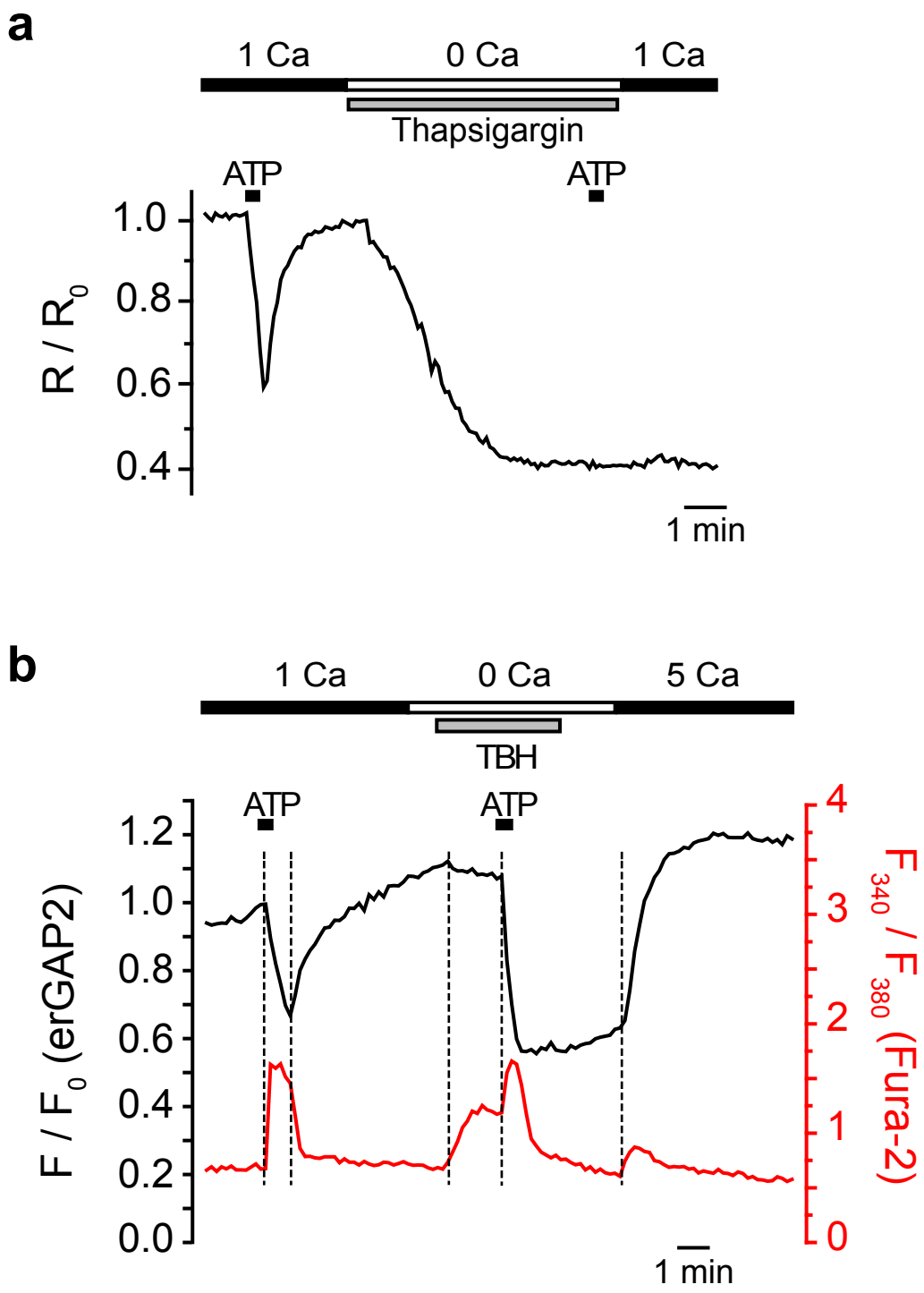
a
1 Ca
0 Ca
1 Ca
Thapsigargin
ATP
ATP
1.0
0.8
0.6
0.4
R / R0
1 min
b
1 Ca
0 Ca
5 Ca
TBH
ATP
ATP
1.2
1.0
0.8
0.6
0.4
0.2
0.0
F / F0 (erGAP2)
4
3
2
1
0
F340 / F380 (Fura-2)
1 min

Fig. S3

a

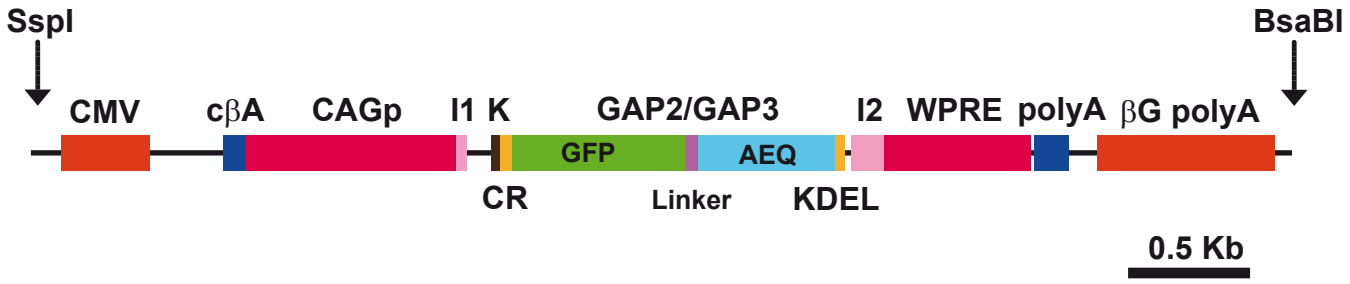
SspI
BsaBI
CMV
cβA
CAGp
I1
K
GAP2/GAP3
I2
WPRE
polyA
βG polyA
GFP
AEQ
CR
Linker
KDEL
0.5 Kb

b

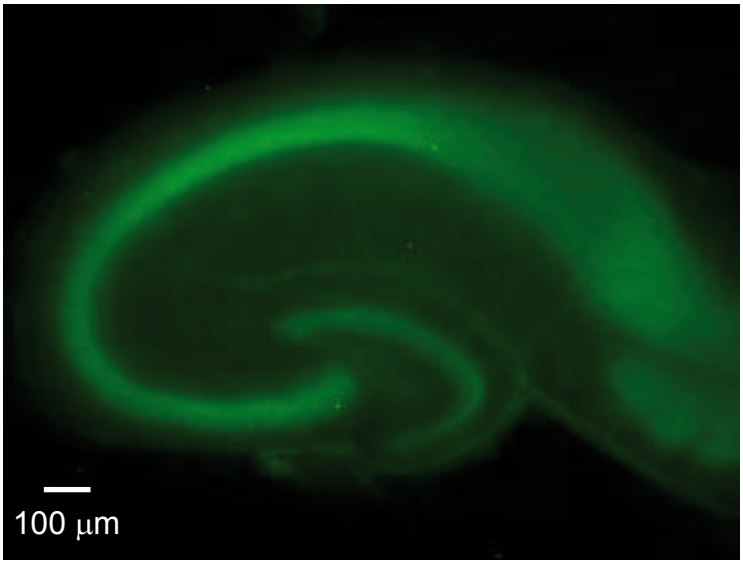
100 μm

Fig. S4

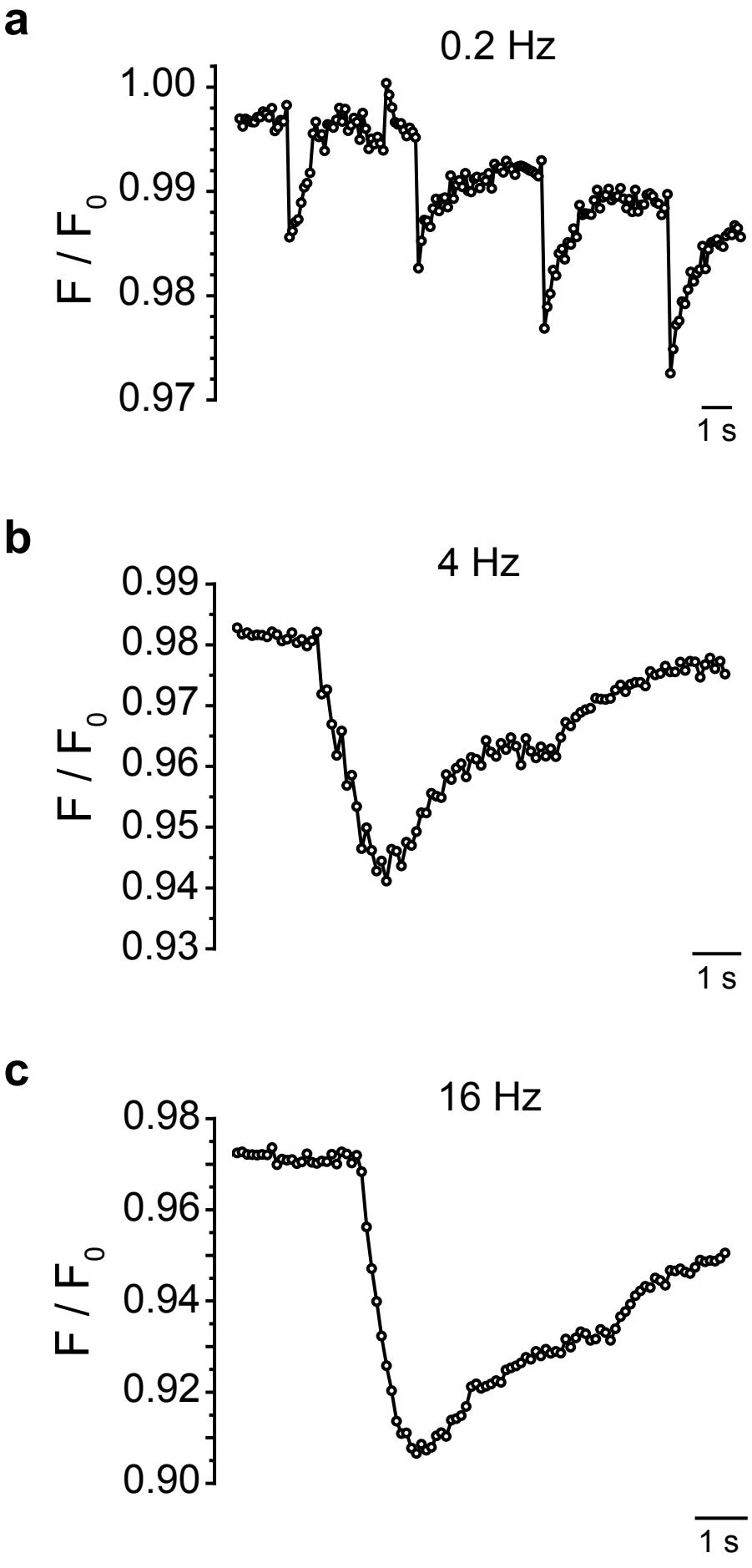
a
0.2 Hz
1.00
0.99
0.98
0.97
F / F0
1 s
b
4 Hz
0.99
0.98
0.97
0.96
0.95
0.94
0.93
F / F0
1 s
c
16 Hz
0.98
0.96
0.94
0.92
0.90
F / F0
1 s

Click here to access/download

Supplemental Movies & Spreadsheets

Video1_OscilGlia_erGAP.gif

Click here to access/download

Supplemental Movies & Spreadsheets

Video2_GAP&Rhod.gif